Rescaling invariance and anomalous energy transport
in a small vertical column of grains

A. Gnoli[1], G. Pontuale[2], A. Puglisi[1] and A. Petri[1,3*]

[1]*CNR-Istituto Sistemi Complessi, Dipartimento di Fisica,*
Università Sapienza, P.le A. Moro, I-00185 Rome, Italy
[2]*Council for Agricultural Research and Economics (CREA-FL),*
Via Valle della Quistione 27, I-00166 Rome, Italy and
[3] *Enrico Fermi Research Center (CREF), via Panisperna 89A, 00184 Rome, Italy*

It is well known that energy dissipation and finite size can deeply affect the dynamics of granular matter, often making usual hydrodynamic approaches problematic. Here we report on the experimental investigation of a small model system, made of ten beads constrained into a 1-d geometry by a narrow vertical pipe and shaken at the base by a piston excited by a periodic wave. Recording the beads motion with high frame rate camera allows to investigate in detail the microscopic dynamics and test hydrodynamic and kinetic models. Varying the energy we explore different regimes from fully fluidized to the edge of condensation, observing good hydrodynamic behavior down to the edge of fluidization, despite the small system size. Density and temperature fields for different system energies can be collapsed by suitable space and time rescaling, and the expected constitutive equation holds very well when the particle diameter is considered. At the same time the balance between dissipated and fed energy is not well described by commonly adopted dependence, due to the up-down symmetry breaking. Our observations, supported by the measured particle velocity distributions, show a different phenomenological temperature dependence, which yields equation solutions in agreement with experimental results.

I.   I. INTRODUCTION

Granular matter can display a variety of behaviors [1, 2], from quasi-solid to fluid-like states, for which effective descriptions exist in a limited number of regimes. At the same time it is also a paradigmatic representation of a dissipative system far from equilibrium and as such it is often explored as a model system. In the absence of external forces grain motion, even if initially present, eventually comes to an end because of the inelastic and frictional interparticle collisions. Otherwise it can be sustained by continuous energy supply. Among many others, a main issue is whether and within which limits such situations can be described by hydrodynamics, where that granularity disappears and the system state is defined by continuous fields in terms of local averages of quantities like velocity, granular temperature and density.

Hydrodynamic descriptions of granular flow have been developed with some success (see e.g. the reviews in [3, 4]). Being evident the advantages of such a description, it can fail for several reasons. Among them, besides the discrete nature of the system components, there is the energy dissipation due to intergrain collisions and friction, that can generate strong gradients and space-velocity correlations and lead to clusterization [5–8]. To this respect it is critical the way in which energy is fed [8], since it strongly influences dynamics through the way energy is redistributed [6]. But also a homogeneous fluidized state can become unstable with respect to small density perturbations and evolve so that a dilute granular fluid co-exists with much denser solid-like clusters [9]. To address such situations it is often necessary to introduce more complex quantities, like variable viscosity, additive diffusive terms etc. [4], making applications problematic in several circumstances and stimulating the formulation of computational methods based on effective interaction terms, like e.g. smoothed-particle hydrodynamics [10–12].

Granular hydrodynamics can represent a problem even in one dimension, as shown in the seminal work by Li and Kadanoff [6] where a system can end in a static state because grains clusterize far from the energy source. One-dimensional systems are important also for the understanding of granular hydrodynamics in higher dimension, as stressed by Sela and Goldhrisch [7]. In addition, 1–d and quasi-1–d granular systems represent simplified situations to investigate phenomena, like e.g. wave transmission [13–16]. Their properties can be of some relevance in the field of active matter, where one dimensional systems are often considered [17–23], and interesting for applications, as for instance in granular dampers [24, 25].

Most of work on granular hydrodynamics is based on calculations and numerical simulations, with sometimes disagreeing conclusions. In 1–d hydrodynamics has been studied analytically under various conditions and different

ways of feeding energy, generally for well fluidized, and large systems [7, 26–31], stimulating a number of simulations [5–8, 27, 31–45]. There are very few experimental works that, rather than verifying hydrodynamic behavior, are generally mainly focused on collective dynamics and specific phenomena, like inversions or Leidenfrost effects, among them [35, 46–51].

Far from giving a general description, our work aims at testing hydrodynamics experimentally in the simple case of small 1–d systems in a statistically stationary state. As remarked above, similar systems have been subject of several studies from the theoretical and numerical point of view, but very few experimental instances can be found. Despite the unavoidable limits of the experimental conditions, this work aims at broadening the knowledge of the field by providing an experimental demonstration that even a small system of grains is very well described in terms of continuous hydrodynamic density and temperature fields with well defined properties.

In the following, Sec. II is devoted to describe the experiment and its parameters, anticipating that the field profiles observed for different system energies can all be overlapped by suitable time and space rescaling. Measured hydrodynamic fields are shown in Sec. III, where a state equation of the Van der Waals type is successfully tested. In Sec. IV, energy dissipation and current are experimentally measured, finding that the latter does not agree with what resulting from its expression usually adopted in terms of field. On the base of experimental observations a different expression for the temperature dependence is formulated, which is also connected with the asymmetry induced by gravity in the velocity distribution of the grains. In Sec. V this expression is employed in the hydrodynamic equations, yielding solutions in agreement with the observed fields. Final considerations are contained in Sec. VI, while more experimental and procedural details can be found in the Supplementary Information (SI).

II.   II. EXPERIMENTAL PARAMETERS AND RESCALING

We have investigated a set of N=10 identical steel beads of diameter $d = 4$ mm, restitution coefficient $\epsilon \simeq 0.92$, constrained to move in a vertical pipe (Fig. S1 in SI). The energy is supplied to the system by a oscillating piston that hits vertically the lowest grain, and gravity prevents to reach absorbing states with collapsed grains. Changing the amount of fed energy allows to explore different regimes. The piston is driven sinusoidally at a frequency $f = 30$ Hz, and the grain motion is recorded by a video camera at 480 fps and digital images are processed to reconstruct the trajectories of the center of mass of each bead (see SI). Being collisions substantially central, spin motion has not been taken into account. In the following, lengths and times will be converted from pixel and frames into millimeters and seconds, and the grain mass will be taken adimensional and set equal to 1 (experimental and data processing details are available in the SI).

Here we report on a series of 7 experiments in which the piston amplitude varies from $A = 2.90$ mm to $A = 1.15$ mm, with corresponding driving temperatures $T_0 = (2\pi f A)^2$ reported in Tab. I. This choice of parameters allows to explore the behavior of the system from well fluidized to almost collapsed states.

Set S	1	2	3	4	5	6	7
T_0 (mm/s)$^2 \cdot 10^4$	30.22	28.52	22.20	16.67	14.21	9.86	4.82
λ (mm)	70.8	69.1	62.6	57.0	54.5	50.1	44.9
τ (s) $\cdot 10^{-2}$	8.85	8.84	7.99	7.62	7.45	7.14	6.77

TABLE I. Values of temperatures characterizing the piston motion in the experiments considered here.

In hydrodynamics, generic (e.g. dimensional) considerations usually allow one to identify several length and time scales characterizing the system, such that different systems may display the same dynamics after suitable rescaling of the fields. This expectation has been extended to granular systems but it is difficult to prove on a general foot, due to the huge number of possible granular regimes. For specific systems like that at hand, characteristic scales have been introduced in theoretical approaches [31, 32, 42].
A first important attainment of the present work is to show that fields observed at different T_0 can be collapsed to a same profile if the finite size of the particles is taken into account in a suitable way. There are different relevant scales in the system. In the present case, being the supplied energy the varying parameter, the relevant space and time scales (remind that $m = 1$) are related to the source temperature T_0, and without loss of generality can be taken respectively proportional to $\lambda = T_0/g$ and $\tau = \sqrt{\lambda/g}$ [26, 31]. However, experimental data show that in the present case this choice does not produce a good field collapse, which instead, is obtained rescaling by

$$\lambda = T_0/g + Nd, \tag{1}$$

which implicitly modifies also τ. Such dependence appears natural since , taken two bead columns at rest made of different number N with different diameter d (identical in each column), they can be made look the same by

measuring space in units of length Nd. We test the validity of this expression in the following by considering the rescaled fields. Notice that also $\tau = \lambda/\sqrt{T_0}$ is a possible definition. The two choices for τ, respectively inertial and ballistic, coincide only for $d = 0$ but in the present case the second choice performs worse.

III. III. HYDRODYNAMIC DESCRIPTION AND FIELDS

Derivation of hydrodynamic equations for granular flow has been performed in different ways, situations, and dimensions (see eg. [2] and refs. therein). In their general form they are akin to those for true fluids but also account for the energy dissipated in collisions. Naming z the only coordinate, they have the form:

$$\partial_t \rho = -\partial_z(\rho v) \tag{2}$$
$$\rho\,\partial_t u = -\rho u \partial_z u - \rho g + \partial_z P \tag{3}$$
$$\rho\,\partial_t T = -\rho u \partial_z T - \partial_z J - P\partial_z u - W, \tag{4}$$

where $u(z,t)$ and $\rho(z,t)$ are the velocity and density fields, $T(z,t)$ and $P(z,t)$ temperature and pressure, g the gravity acceleration. These equations respectively describe mass conservation, momentum conservation (Euler equation) and energy balance. Here W is the rate of energy density dissipated in collisions and J the energy current through the system. In the stationary state the first equation is trivially satisfied, and the others dry to

$$\partial_z P - \rho g = 0 \tag{5}$$
$$\partial_z J - W = 0 \tag{6}$$

corresponding respectively to the Stevino's law and to a continuity equation for the energy density. Suitable boundary conditions and constitutive relations are necessary to make closed the theory. Both ingredients are unknown in general. A main outcome of our study is the proposal of constitutive relations for pressure, energy current and dissipation rate.

In order to verify experimentally Eqs. (5) and (6) local stationary fields $\rho(z), v(z)$ and $T(z)$ have been evaluated from the video recordings (see SI). Figure 1 shows the densities ρ (top) and temperature T (bottom) fields for the different sets considered. The main panels report the rescaled quantities: $\rho \to \rho\lambda$, $T \to T\tau^2/\lambda^2$, as functions of the rescaled height $z \to z/\lambda$. A good similarity is obtained for most of the cases: the fields appear rather smooth for sets of higher energy, while granularity becomes visible for decreasing T_0, especially in sets S6 and S7. Density is very constant in the system bulk, displaying rather well equispaced relative maxima with symmetric shape in less fluidized systems, where also increases close to the piston because of the low bead kinetic energy. Rescaled temperatures decay about linearly far enough from the piston, displaying a common pattern in regions of increasing size for increasing set energy, sign that rescaling of hydrodynamics holds also for this granular systems if particle diameter is suitably considered and system is fluid enough. Non rescaled densities and temperatures are plotted for comparison in the inset of the respective figures, showing real spatial extension and temperatures of the systems.

An important point concerns the system boundaries where particular conditions act. On one side there is the energy source which affects the dynamics of the bottom particle, and consequently the fields in that region. On the other hand, the top particle is free to jump and could deserve a separate ballistic dynamical description [26], but in the present case it does not show particular anomalies. It appears that the piston motion affects some quantities. For instance, density and temperature vanish approaching z = 0 (Fig. 1), signaling a region of rarefaction and one can expect hydrodynamics to not hold in that region. However, it must be noticed other quantities seem not affected, like pressure (Fig. 2).

IV. IV. CONSTITUTIVE EQUATIONS

From a variety of arguments (see e. g. [7, 26, 52]) one expects that in dilute situations the pressure P follows: $P(z) = \rho(z)T(z)$, namely it is proportional to the "internal" energy, like in a perfect gas. However, as anticipated, the finite diameter of the beads represents an important issue that must be considered, like in the Van der Waals equation. An instance where it happens is represented by the 1–d Tonks gas of hard rods [53], where pressure has the expression:

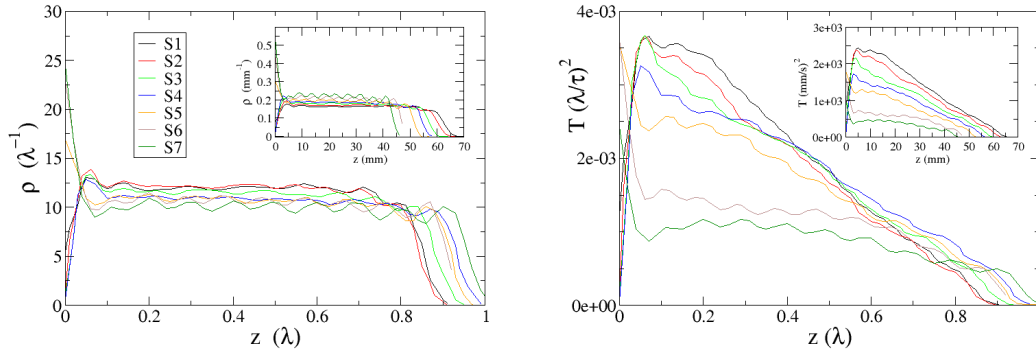$$P_d(z) = \frac{P(z)}{1 - \frac{\rho(z)}{\rho_c}}, \tag{7}$$

FIG. 1. Density (top) and temperature (bottom) profiles rescaled by the characteristic scales λ and τ. Strong bead localization is visible at low energy.

with $\rho_c = \frac{N}{Nd} = \frac{1}{d}$. A similar expression has been derived for a 1–d model granular system [39]. The main panel of Fig. 2 shows this quantity vs $P_S = g \int_z^\infty \rho(z)dz$, as suggested by Eq. (5). Both quantities are rescaled according to τ^2/λ. It is seen that pressure behaves smoothly and follows a linear trend in more energetic systems, while in low energy systems display granularity, reflecting in large fluctuations which however do not change the average behavior. Notice that since the quantities on the two axes have the same dimension, the slope of the curves, which turns out to be $\simeq 10^{-2}$, do not depend on T_0 even without rescaling. The importance of accounting for the finite diameter is demonstrated in the inset of Fig. 2, where $P(z) = \rho(z)T(z)$ is plotted instead of P_d resulting in a different slope for each set.

Slightly different formulations can be found for the explicit expressions of W and J in Eq. (6). From kinematic arguments one expects [6, 31] $W = C_1(1 - \epsilon^2)\rho^2 T^{3/2}$, where C_1 is an adimensional constant. This expression neglects velocity-position correlations, which have been observed to invalidate it in some simulations [54]. Moreover, it has to suitably modify it to account for the finite particle diameter. Following the derivation, it is easy to see that the modified expression reads:

$$W = C_1(1 - \epsilon^2)\frac{\rho^2 T^{3/2}}{1 - \rho d}, \tag{8}$$

similarly to other cases.

We have tested the expression (8) by considering an explicit microscopic measure of the energy current [55], which has its simple justification also in considering ρT as a kinetic charge and multiplying it with its velocity v, as usual:

$$J(z) = C_2 \rho(z)\langle v^3(z)\rangle. \tag{9}$$

Evaluation of the constants C_1 and C_2 requires a detailed description of the kinetics and the related statistics, and is strongly dependent on a series of assumptions. Here we only adopt arbitrary values when necessary to compare different quantities. To avoid the noise consequent to differentiation, we have integrated Eq. (6) with the boundary condition $J(\infty) = 0$. Moreover, being unknown whether J can actually be expressed in terms of fields, we have considered non rescaled quantities. The results for all the experimental sets are shown in Fig. 3, where $W_c = \int_\infty^z W(z')dz'$. Apart from a multiplicative constant the two quantities look to display rather close behavior far enough from the bottom. This is especially true for more energetic sets, where the curves are closer in a wider range, down near the energy source, indicating that the expression for W in terms of fields taking into account the particle size, works to a good extent. The values of C_2/C_1 employed to make the two quantities comparably match range from ≈ 1.1 for S1 to ≈ 3.8 for S7.

Constitutive expressions relating the current J with the fields have been obtained in various circumstances. A natural expression, for small gradients, is

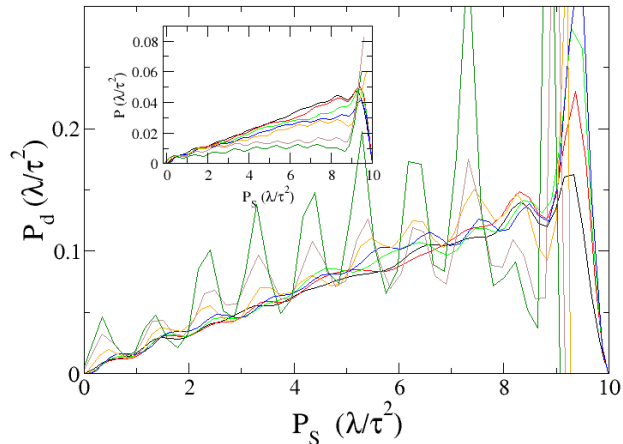$$J = \kappa\frac{\partial T}{\partial z} + \mu\frac{\partial \rho}{\partial z} \tag{10}$$

FIG. 2. Main panel: Test of Van der Waals-Tonks gas expression for pressure, P_d (Eq. 5), vs the Stevino's law; Inset: the same using $P(z) = \rho(z)T(z)$ insted of P_d.

with $\kappa \simeq \mu \propto T^{\frac{1}{2}}$. We checked that this expression does not work in the present case, as can be also easily seen by considering that, far enough from the piston, $T \simeq 1 - const \cdot z$ and $\rho \simeq const$ yield $J \approx (1 - const \cdot z)^{\frac{1}{2}}$, well different from the curves in Fig. 3.

Expression (10) can be obtained by simple arguments [26]. More refined derivations based on a Chapman-Enskog expansion [2, 55, 56], which aims at expressing the local Probability Distribution of Velocity (PDV) in terms of the other fields by expanding small fluctuations, around a homogeneous solution, in terms of powers of the fields gradients. To find explicit expressions for the resulting coefficients, the PDV is then usually expressed in terms of polynomials that can account only for not too large perturbation of the Gauss-Maxwell distribution. Moreover, polynomials are generally taken as functions of v^2, assuming a symmetrical PDV in force of the homogeneity and isotropy. The present one is of course not the case. Gravity and the way of supplying energy break isotropy, enforcing a strong and permanent asymmetry of the PDV, as shown in Fig. 3 where in order to maintain the energy balance the third moment of velocity looks persistent almost everywhere.
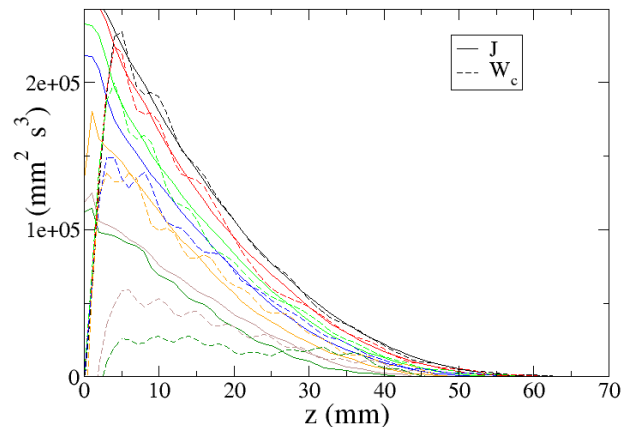

FIG. 3. Comparison of the cumulated dissipated energy rate $W_c = \int W dz$ from Eq. (8) a with the energy current J (see text).

This is confirmed by Fig. 4, where the local PDV $p(z, v)$ evaluated from experimental data of set S1 is shown. Large
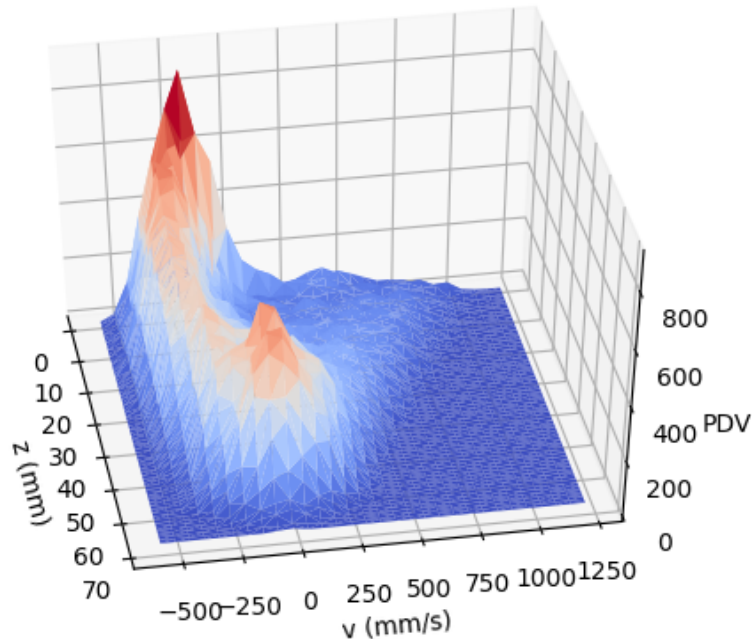
FIG. 4. Probability distribution of the velocity field for the set S1.

asymmetries are seen. As can be expected from the behavior of J, they decrease towards the top of the column, but it can be verified that the velocity distributions are not Gaussian for any of the particle, even in almost symmetrical cases. This feature is shared by all the experimental sets, including low energy ones, where asymmetry is weaker. It is also seen that close to the bottom the distribution is bimodal, a feature that could be spuriously due to the proximity of the piston, as already observed in different experiments [47].

V.   V. PHENOMENOLOGICAL DESCRIPTION

These last observations make problematic the description of the system in terms of usual hydrodynamics fields ρ, u and T. Starting from a Gaussian PDV, asymmetries can be accounted in some cases by additional fields, like for instance in [7]. However this is not always possible, like for instance in the presence of shear [4]. A different approach consists in considering the possibility that, despite the "anormal" PDV, current could be expressed in terms of the usual fields, although in not immediate way. In this perspective it is of help to observe that as far as $J \simeq W_c$ then $J \approx T^{\frac{5}{2}}$. In fact one can see that, at least far enough from the bottom, from Fig. 1 one can assume $dT/dz \simeq const$, and hence $W_c = \int W dz = \int W dT \frac{dz}{dT} \approx T^{\frac{5}{2}}$.

This looks at first sight weird, since from $J \propto \rho < v^3 >$ and $\rho \simeq const$, one would expect $J \approx T^{\frac{3}{2}}$. This implicitly assumes a linear dependence of the exponents characterizing different moments: $< v^q > \propto T^{\frac{q}{2}}$, which is not the case here. Notice that J is close to W_c in a wide range of z that increases down to $z \approx 5$ mm in most energetic sets, implying a determinate, although non linear, dependence between the exponents of different moments of the PDV for a wide range of temperatures. This can be surprising since in Fig. 4 PDV looks to change substantially in this range.

To test whether $J \approx T^{5/2}$ is a reasonable guess, we use it in the hydrodynamic equations where, for such heuristic argument, we neglect the excluded volume. We also move to the Lagrangian frame where equations take a simpler
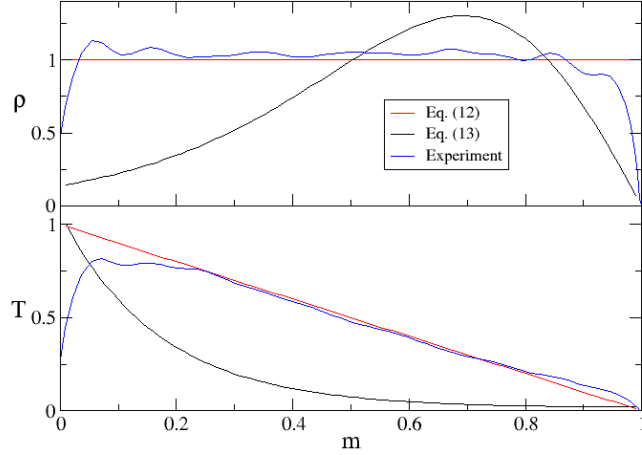
FIG. 5. Experimentally observed density and temperature fields (set S1), compared with the solutions of usual stationary equation (14), and the alternative form (13) (fields are expressed in the Lagrangian coordinate and multiplied by arbitrary constants to ease the comparison).

form. After rescaling by λ and τ (with $d = 0$), transforming to the variable $y = \int_0^z \rho(z')dz'$ yields [31]:

$$\rho T = (1 - y) \tag{11}$$

$$\rho \frac{\partial J}{\partial y} = W. \tag{12}$$

Taking $J \propto \rho T^{\frac{5}{2}}$ and $W \propto \rho^2 T^{\frac{3}{2}}$, eliminating ρ through Eq. (11) yields:

$$\frac{\partial (1 - y)T^{\frac{3}{2}}}{\partial y} = C(1 - y)T^{\frac{1}{2}}, \tag{13}$$

where C is some proportionality constant. It is straightforward to see that from the boundary condition $T(1) = 0$ it follows $T \propto (1 - y)$ and consequently, from Eq. (11), $\rho(y) \propto cost$. These solutions qualitatively well agree with the experimental observations. It can be worth mentioning that in [35] some results from simulations with identical N and ϵ, and $f = 20$ Hz, also show a linearly decaying temperature (see Fig. 5b) therein). Density is seen to decreases from bottom up (Fig. 5a)), but with a trend to become more uniform for increasing T_0.

In order to compare our results with what expected from usual approaches [57] we have considered the equation [30, 31]:

$$\frac{\partial (1 - y)T^{\frac{1}{2}}}{\partial y} = \Lambda^2 (1 - y)T^{\frac{1}{2}}, \tag{14}$$

whose solutions , with the boundary condition $dT/dy = 0$ at $y = 1$ can be expressed through the modified Bessel function of the first kind $I_0(x)$ as

$$T(y) = \frac{I_0^2(\Lambda(1 - y))}{I_0^2(\Lambda)}.$$

Here $\Lambda = \frac{N\sqrt{\pi(1-\epsilon^2)}}{2}$ which in our case is $\simeq 3.47$. The resulting field profiles are reported in Fig. 5 together with the solutions of Eq. (13) and those observed experimentally for set S1, confirming that the usual field dependence of the energy current does not account for our observations, which are instead reproduced by the proposed form.

VI.   VI. DISCUSSION AND CONCLUSIONS

The results here reported demonstrate that gravity is an efficient energy redistributor, but also a symmetry breaking factor which produces persistent asymmetry of the velocity probability function in the stationary state, that we have measure experimentally. Such asymmetry can be expected to persist also in higher dimension, and in larger systems, since it is essential to sustain the upward energy flux, and it should indeed increase because of the increasing dissipation. On the other hand it had already been shown that hydrodynamic description must include asymmetry even in the absence of symmetry breaking [7].

The energy flux measured in the system is different from what expected by usual theories. Adopting a phenomenological expression derived from observations, we have found solutions of the hydrodynamic equations in agreement with the experimental results.

A standard constitutive equation, that accounts for the finite bead diameter, has been observed to be well verified (in average even in systems at the edge of condensation). While this had been predicted by some granular theories, it had not yet been experimentally observed. Finally, experiments show that many quantities can be rescaled by a characteristic length tied to Nd. This result and the finite diameter correction in the constitutive equation, as in other quantities, are expected to hold also for larger and higher dimensional similar systems, i.e. stacks of beads shaken from the bottom under gravity, provided that - in the directions perpendicular to the gravity - there are no inhomogeneities or instabilities such as convection etc. On the contrary, the expression adopted for the flux energy and the observed fields could be specific of the particular system investigated, and different in larger and higher dimensional systems. Nevertheless they bring about the lack of theory for systems like the one considered here, and the necessity of considering odd moments of the velocity distribution.

[1] H. M. Jaeger, S. R. Nagel, and R. P. Behringer, Phys. Today **49**, 32 (1996).
[2] A. Puglisi, *Transport and Fluctuations in Granular Fluids* (Springer, 2014).
[3] I. Goldhirsch, Annual Review of Fluid Mechanics **35**, 267 (2003).
[4] C. S. Campbell, Powder Technology **162**, 208 (2006).
[5] S. Mc Namara and W. Young, Phys. Fluids A **5**, 34 (1993).
[6] Y. Du, H. Li, and L. P. Kadanoff, Phys. Rev. Lett. **74**, 1268 (1995).
[7] N. Sela and I. Goldhrisch, Phys. Fluids **7**, 507 (1995).
[8] A. Puglisi, V. Loreto, U. M. B. Marconi, A. Petri, and A. Vulpiani, Phys. Rev. Lett. **81**, 3848 (1998).
[9] F. Lu, C. Zhang, Y. Wang, W. Qian, and F. Wei, Particle technology and fluidization **68**, 17530 (2022).
[10] K. Szewc, Granular Matter **19**, 3 (2016).
[11] C. Zhang, Y.-j. Zhu, D. Wu, N. A. Adams, and X. Hu, Journal of Hydrodynamics **34**, 767 (2022).
[12] F. Xu, J. Wang, Y. Yang, L. Wang, Z. Dai, and R. Han, Acta Mechanica Sinica **39**, 722185 (2023).
[13] A. Misra and N. Nejadsadeghi, Wave Motion **90**, 175 (2019).
[14] K. Taghizadeh, H. Steeb, and S. Luding, EPJ Web of Conferences: Powders and Grains 2021 **249** (2021).
[15] W. Zhang and J. Xu, Extreme Mechanics Letters **43**, 101156 (2021).
[16] T. Jiao, S. Zhang, M. Sun, and D. Huang, Nonlinear Dynamics **111**, 9049 (2023).
[17] E. Locatelli, F. Baldovin, E. Orlandini, and M. Pierno, Phys. Rev. E **91**, 022109 (2015).
[18] L. Barberis and F. Peruani, J. Chem. Phys. **150**, 144905 (2019).
[19] P. Dolai, A. Das, A. Kundu, C. D. A. Dhar, and K. V. Kumar, Soft Matter **16**, 7077 (2020).
[20] P. Illien, C. de Blois, Y. Liu, M. N. van der Linden, and O. Dauchot, Phys. Rev. E **101**, 040602 (2020).
[21] M. Bär, R. Großmann, S. Heidenreich, and F. Peruani, Annual Review of Condensed Matter Physics **11**, 441 (2020).
[22] L. Caprini and U. M. B. Marconi, Phys. Rev. Res. **2**, 033518 (2020).
[23] T. Banerjee, R. L. Jack, and M. E. Cates, Journal of Statistical Mechanics: Theory and Experiment **2022**, 013209 (2022).
[24] M. Ferreyra, M. Baldini, L. Pugnaloni, and S. Job, Granular Matter **23**, 1 (2021).
[25] Z. Zhou, D. M. McFarland, X. Cheng, H. Lu, and A. F. Vakakis, Nonlinear Dynamics **111**, 14713 (2023).
[26] P. K. Haff, J. Fluid Mech. **134**, 401 (1983).
[27] E. L. Grossman and B. Roman, Physics of Fluids **8**, 3218 (1996).
[28] E. L. Grossman, T. Zhou, and E. Ben-Naim, Phys. Rev. E **55**, 4200 (1997).
[29] R. Ramírez and P. Cordero, Phys. Rev. E **59**, 656 (1999).
[30] J. J. Brey, M. J. Ruiz-Montero, and F. Moreno, Phys. Rev. E **63**, 1 (2001).
[31] Y. Bromberg, E. Livne, and B. Meerson, in *Granular Gas Dynamics*, Lect. Notes Phys., Vol. 624, edited by T. Thorsten Pöschel and N. V. Brilliantov (Springer, Springer, Berlin, Heidelberg, 2003) pp. 251–266.
[32] B. Bernu, F. Delyon, and R. Mazighi, Phys. Rev. E **50**, 4551 (1994).
[33] L. P. Kadanoff, Rev. Mod. Phys. **71**, 435 (1999).
[34] I. Goldhrisch, Chaos **9**, 659 (1999).
[35] S. Luding, E. Clément, A. Blumen, J. Rajchenbach, and J. Duran, Phys. Rev. E **49**, 1634 (1994).

[36] R. Soto and M. Mareschal, Phys. Rev. Lett. **83**, 5003 (1999).
[37] A. Alexeev, A. Goldshtein, and M. Shapiro, Powd. Tech. **123**, 83 (2001).
[38] A. Baldassarri, U. M. B. Marconi, A. Puglisi, and A. Vulpiani, Phys. Rev. E **64**, 011301 (2001).
[39] F. Cecconi, F. Diotallevi, U. M. B. Marconi, and A. Puglisi, J. Chem. Phys. **120**, 35 (2004).
[40] J. A. Carrillo, T. Pöschel, and C. Salueña, J. Fluid Mech. **597**, 119–144 (2008).
[41] M. V. Carneiro, J. J. Barroso, and E. E. N. Macau, Math. Probl. Eng. **2009**, 345947 (2009).
[42] P. Eshuis, K. Van Der Weele, E. Calzavarini, D. Lohse, and D. Van Der Meer, Phys. Rev. E **80**, 1 (2009).
[43] D. Denis Blackmore, R. Anthony, X. Tricoche, K. Urban, and L. Zou, Phys. D **273-274**, 14 (2014).
[44] C. R. Windows-Yule, D. L. Blackmore, and A. D. Rosato, Phys. Rev. E **96**, 1 (2017).
[45] A. Baldassarri, A. Puglisi, and A. Prados, Phys. Rev. E **97**, 062905 (2018).
[46] L. Bocquet, W. Losert, D. Schalk, T. C. Lubensky, and J. P. Gollub, Phys. Rev. E **65**, 011307 (2001).
[47] J. A. Perez, S. B. Kachuck, and G. A. Voth, Phys. Rev. E **78**, 1 (2008).
[48] C. G. Johnson and J. M. N. T. Gray, J. Fluid Mech. **675**, 87–116 (2011).
[49] G. Lumay, S. Dorbolo, O. Gerasymov, and N. Vandewalle, Eur. Phys. J. E: Soft Matter Biol. Phys. **36**, 16 (2013).
[50] G. Pontuale, A. Gnoli, F. V. Reyes, and A. Puglisi, Phys. Rev. Lett. **117**, 098006 (2016).
[51] L. Oyarte Gálvez, N. Rivas, and D. van der Meer, Phys. Rev. E **97**, 042901 (2018).
[52] C. S. Campbell, Annu. Rev. Fluid Mech. **22**, 57 (1990).
[53] L. Tonks, Phys. Rev. **50**, 955 (1936).
[54] N. Mitarai and H. Nakanishi, Physical Review E - Statistical, Nonlinear, and Soft Matter Physics **75**, 1 (2007).
[55] V. Garzo and J. Dufty, Phys. Rev. E **59**, 5895 (1999).
[56] J. Brey, J. Dufty, C. Sub Kim, and A. Santos, Phys. Rev. E **58**, 4638 (1998).
[57] It can be worth remarking that slightly different equations can be derived, depending on the form of thermal conductivity.